

## The Effects of Charges at the N- and C-Termini of Short Peptides on Their Secondary and Self-assembled Structures

Kin-ya Tomizaki,<sup>\*1,2</sup> Tomoyo Ikawa,<sup>2</sup> Soo-Ang Ahn,<sup>2</sup> Seiji Yamazoe,<sup>1,2</sup> and Takahito Imai<sup>2</sup>

<sup>1</sup>Innovative Materials and Processing Research Center, Ryukoku University, Seta, Otsu, Shiga 520-2194

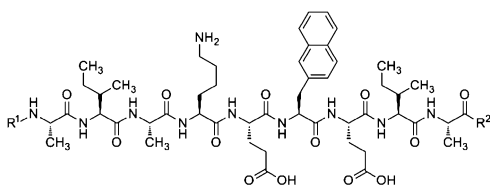
<sup>2</sup>Department of Materials Chemistry, Ryukoku University, Seta, Otsu, Shiga 520-2194

(Received March 3, 2012; CL-120184; E-mail: tomizaki@rins.ryukoku.ac.jp)

Self-assembly of small molecules (i.e., synthetic peptides) into nanostructures is an attractive template for fabrication of nanoscaled organic–inorganic composites. In order to increase the diversity of morphologies of template nanostructures, we designed, synthesized, and characterized four different nonapeptides, and examined the effects of charge(s) at the N- and/or C-termini of the peptides on their secondary and assembled structures in water.

Self-assembly of small molecules into nanostructures is an attractive bottom-up approach for the fabrication of nanoscaled functional materials.<sup>1–4</sup> Peptides are relatively easy to design and synthesize, and can form secondary structural elements of proteins such as  $\alpha$ -helices,  $\beta$ -sheets, turns, and loops. So far, great efforts have been devoted to the use of self-assembled nanostructures of synthetic peptides as building blocks.<sup>5–18</sup> In this context, we are now focusing on the use of peptide assemblies as templates to fabricate well-organized organic–inorganic composites. A key element for peptide-directed mineralization is to increase the diversity of the morphologies of template nanostructures. In our previous study, we designed, synthesized, and characterized self-assembled peptide nanostructures, where amphiphilic nonapeptides showed a pH-dependent morphology change.<sup>19</sup> Thus, we herein describe the effects of the N- and/or C-terminal charge(s) of a nonapeptide on the morphology of assembled nanostructures in water.

Amphiphilic nonapeptides **P1–P4** were basically designed based on the amino acid sequence of **RU-002**<sup>19</sup> to have two isoleucines (Ile) and a 2-naphthylalanine [Nal(2)] at one face, which provides the driving force for self-assembly via hydrophobic interactions (Figure 1). Three alanines (Ala) and two glutamic acids (Glu) were placed at another face to make the peptides water-soluble. In particular, the Glu residues were



Peptide	R <sup>1</sup>	R <sup>2</sup>
<b>P1</b> (RU-011):	H	NH <sub>2</sub>
<b>P2</b> (RU-012):	Ac	OH
<b>P3</b> (RU-013):	H	OH
<b>P4</b> (RU-004):	Ac	NH <sub>2</sub>

**Figure 1.** Amino acid sequences of the nine-residue peptides, **P1**, **P2**, **P3**, and **P4**, used in this study.

arranged at the C-terminal half within the sequence favorable to form an antiparallel  $\beta$ -sheet structure (and/or destabilize a parallel alignment by charge repulsions among the Glu side chains). In **P1**, the C-terminus was protected with an amide; **P2** had its N-terminus capped with an acetyl moiety; in **P3**, both N- and C-termini were free to have positively and negatively charged ends, respectively; and both termini of **P4** were capped with acetyl and amide groups, respectively.

Four different peptides were prepared by standard solid-phase peptide synthesis using Fmoc chemistry,<sup>20</sup> purified by reverse-phase HPLC, and characterized by MALDI-TOF-MS. Each peptide stock solution was prepared by dissolving the purified peptide in 2,2,2-trifluoroethanol (TFE) to prevent self-assembly during storage. The concentration of each stock solution was determined by UV–vis spectroscopy using an extinction coefficient of 5500 M<sup>-1</sup> cm<sup>-1</sup> for the Nal(2) residue in aqueous solution containing 1% TFE (v/v).<sup>21</sup> The peptide stock solution in TFE was transferred into a microtube, dried with an N<sub>2</sub> gas stream, then dried in vacuo for 30 min. Ultrapure water (water) was added to the microtube (for peptide-directed mineralization, water as a solvent is necessary to avoid metal contamination) and the obtained aqueous solution was sonicated at 50 °C for 2 min, incubated at 40 °C for 1 day, and then at 25 °C for more than 7 days.

First, the conformational analyses for **P1–P4** were conducted by measuring ATR-FTIR spectra (Shimadzu IR Prestige-21 FT-IR spectrophotometer equipped with Smiths DuraSample IR II, Canada) of peptide films prepared from aqueous solutions of peptides matured in water (Figure 2). The amide I region, originating from the amide carbonyl stretching frequencies between 1600 and 1700 cm<sup>-1</sup>, is often used to assess the amide mode. ATR-FTIR spectra of **P1–P4** revealed that the four different peptides exhibited a strong amide I band around 1625 cm<sup>-1</sup> and a weak band around 1670 cm<sup>-1</sup>, indicating that antiparallel  $\beta$ -sheet conformations were predominant.<sup>22,23</sup> How-

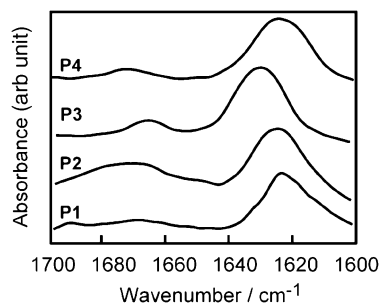


**Figure 2.** ATR-FTIR spectra of peptide films prepared from aqueous solutions of **P1**, **P2**, **P3**, and **P4** matured in water for more than 7 days. ([Peptide] = 1.0 mM in water).

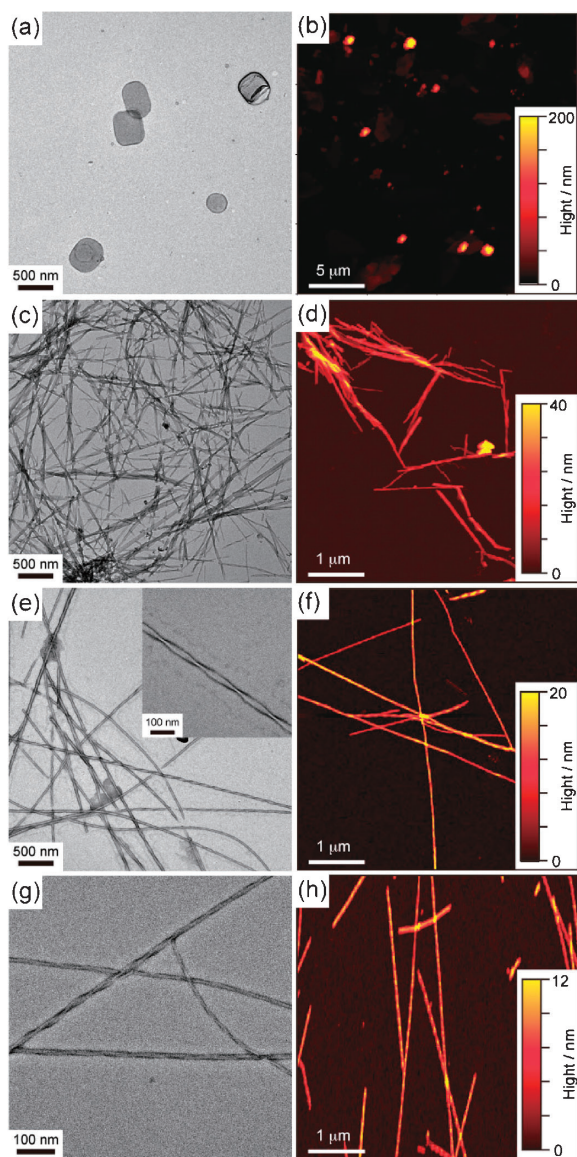


**Figure 3.** TEM (stained by 2% phosphotungstic acid, left column) and tapping-mode AFM images (right column) of **P1** (panels a and b), **P2** (panels c and d), **P3** (panels e and f), and **P4** (panels g and h) matured in water. Inset: TEM image of the expanded area of Figure 3e.

ever, the amide I band for **P3** was observed at a slightly higher wavenumber ( $1630\text{ cm}^{-1}$ ) than those for the others, probably due to loosely assembled peptide backbones in **P3** nanostructures.

Next, we characterized the nanostructures of the peptide assemblies by transmission electron microscopy (TEM, JEOL JEM-2100, Japan) on a collodion membrane-covered Cu grid, and with tapping-mode atomic force microscopy (AFM, Asylum Technologies MFP-3D, Japan) on a Si(100) surface (Figure 3). Figures 3a and 3b show the presence of plate-like, flattened assemblies approximately 500 nm in width and 150 nm in height. No fibrous assemblies were observed there. The peptide assemblies for **P2** were observed to be relatively short, left-handed, loosely twisted ribbon structures approximately 10 nm

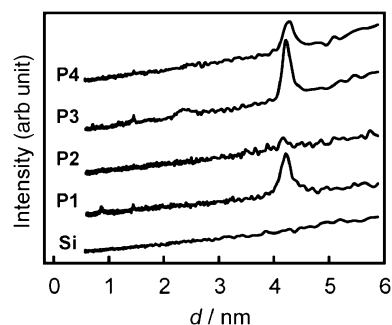


**Figure 4.** XRD patterns of a bare Si(100) substrate as a reference, and peptide films of **P1**, **P2**, **P3**, and **P4** prepared on Si(100) surfaces.

in height and 200 nm in pitch (Figures 3c and 3d). Peptides with charges at both ends, **P3**, assembled into a right-handed fiber formation with heights varying from 10 to 20 nm and approximately 200 nm in pitch (Figures 3e and 3f). Peptides with both ends capped, **P4**, exhibited left-handed straight fibers with a narrow distribution of height (ca. 8 nm) (Figures 3g and 3h).

Differences in morphological features between **P1** and the others likely resulted from the positively charged N-termini of **P1** preventing fibrous formation as seen in our previous work, where **RU-001** peptides with a Glu and two Lys residues at the hydrophilic face formed into a plate-like structure in water.<sup>19</sup> Differences in the directions of coiled fibrils folded into a fiber formation between right-handed **P3** and left-handed **P2/P4** might imply that the terminal charges of **P3** caused not only the mode of hydrogen bonding in the secondary structures, but also the morphology of the self-assembled nanostructures.

In order to understand how peptides were embedded into the self-assembled nanostructures, we acquired X-ray diffraction (XRD, Rigaku RINT2000, Japan) patterns on dry powders for **P1–P4** on Si(100) substrates. The results show significant reflections with the  $d$ -spacing being 4.2 nm, which corresponds closely to the total length of a  $\beta$ -sheet-forming (extended) peptide (Figure 4). The peak at 2.3 nm in the XRD profile for **P3** fits closely the height of a facial hydrophobic interaction between amphiphilic  $\beta$ -sheet-forming peptides. Figure 5 shows a proposed three-dimensional structure of **P3** based on the data obtained from TEM, AFM, and XRD experiments. A representative fiber of **P3** has a right-handed helical coil with dimensions of approximately  $20 \times 20\text{ nm}^2$  as determined by TEM and AFM measurements (Figures 3e and 3f). A rectangular rod having dimensions of  $2.3 \times 4.2\text{ nm}^2$  would be a unit fibril for fiber formation stabilized by electrostatic interactions between the N- and C-termini of peptides in neighboring rectangular rods oriented perpendicular to the fibril axis.

In conclusion, we have examined the effects of terminal charges at the ends of short peptides on their nanostructures. Increasing the number of an amino (positively charged) group in a peptide sequence likely directs plate-like assemblies in water. A Glu-rich peptide programmably assembled into a right-/left-handed fiber formation folded by rectangular unit fibrils. The described peptide nanofibers may be a promising template for biocompatible, designed organic–inorganic hybrid materials.

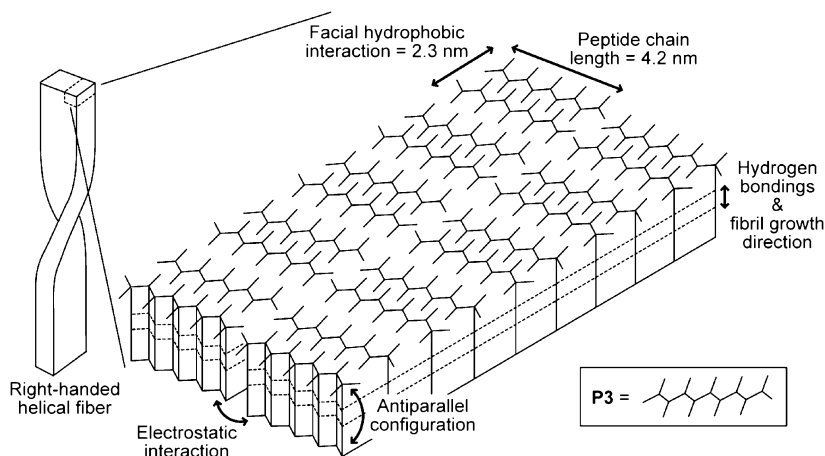


**Figure 5.** Proposed structure of self-assembled **P3** molecules in a fibril.

This study was supported in part by Grants-in-Aid from the Japan Society for the Promotion of Science (JSPS) (K.T.), and the Ryukoku University Science and Technology Fund (K.T.). We thank Professor Hisakazu Mihara (Tokyo Institute of Technology) for assistance with ATR-FTIR measurements.

#### References

- 1 R. V. Uljijn, A. M. Smith, *Chem. Soc. Rev.* **2008**, *37*, 664.
- 2 S. Cavalli, F. Albericio, A. Kros, *Chem. Soc. Rev.* **2010**, *39*, 241.
- 3 R. J. Brea, C. Reiriz, J. R. Granja, *Chem. Soc. Rev.* **2010**, *39*, 1448.
- 4 R. Giraldo, *ChemBioChem* **2010**, *11*, 2347.
- 5 H. Matsui, B. Gologan, *J. Phys. Chem. B* **2000**, *104*, 3383.
- 6 H. Matsui, S. Pan, B. Gologan, S. H. Jonas, *J. Phys. Chem. B* **2000**, *104*, 9576.
- 7 H. Matsui, G. E. Douberly, Jr., *Langmuir* **2001**, *17*, 7918.
- 8 S. Vauthey, S. Santoso, H. Gong, N. Watson, S. Zhang, *Proc. Natl. Acad. Sci. U.S.A.* **2002**, *99*, 5355.
- 9 S. Matsumura, S. Uemura, H. Mihara, *Chem.—Eur. J.* **2004**, *10*, 2789.
- 10 J. R. Lu, S. Perumal, I. Hopkinson, J. R. P. Webster, J. Penfold, W. Hwang, S. Zhang, *J. Am. Chem. Soc.* **2004**, *126*, 8940.
- 11 T. Koga, M. Matsuoka, N. Higashi, *J. Am. Chem. Soc.* **2005**, *127*, 17596.
- 12 H. Yang, M. Pritzker, S. Y. Fung, Y. Sheng, W. Wang, P. Chen, *Langmuir* **2006**, *22*, 8553.
- 13 H. Xu, J. Wang, S. Han, J. Wang, D. Yu, H. Zhang, D. Xia, X. Zhao, T. A. Waigh, J. R. Lu, *Langmuir* **2009**, *25*, 4115.
- 14 H. Cui, T. Muraoka, A. G. Cheetham, S. I. Stupp, *Nano Lett.* **2009**, *9*, 945.
- 15 M. Deng, D. Yu, Y. Hou, Y. Wang, *J. Phys. Chem. B* **2009**, *113*, 8539.
- 16 A. Kholkin, N. Amdursky, I. Bdikin, E. Gazit, G. Rosenman, *ACS Nano* **2010**, *4*, 610.
- 17 V. Castelletto, I. W. Hamley, C. Cenker, U. Olsson, *J. Phys. Chem. B* **2010**, *114*, 8002.
- 18 A. Dhathathreyan, B. U. Nair, *J. Phys. Chem. B* **2010**, *114*, 16650.
- 19 K.-y. Tomizaki, T. Kotera, H. Naito, S. Wakizaka, S.-i. Yamamoto, *Chem. Lett.* **2011**, *40*, 699.
- 20 W. C. Chan, P. D. White, in *Fmoc Solid Phase Peptide Synthesis: A Practical Approach*, ed. by W. C. Chan, P. D. White, Oxford University Press, New York, **2000**, pp. 41–76.
- 21 M. Sadqi, L. J. Lapidus, V. Muñoz, *Proc. Natl. Acad. Sci. U.S.A.* **2003**, *100*, 12117.
- 22 A. Dong, P. Huang, W. S. Caughey, *Biochemistry* **1990**, *29*, 3303.
- 23 S. Srisailam, H.-M. Wang, T. K. S. Kumar, D. Rajalingam, V. Sivaraja, H.-S. Sheu, Y.-C. Chang, C. Yu, *J. Biol. Chem.* **2002**, *277*, 19027.